CRYSTAL GROWTH & DESIGN

pubs.acs.org/crystal

Article

Crystalline Molecular Cleft Clathrates

Published as part of Crystal Growth & Design special issue "Celebrating Mike Ward's Contributions to Molecular Crystal Growth".

Abbie V. Lynch, Toby J. Blundell, and Jonathan W. Steed*

Cite This: *Cryst. Growth Des.* 2024, 24, 7271−7277

Read Online

ACCESS | Metrics & More | Article Recommendations | Supporting Information

ABSTRACT: A rigid bis(urea) molecular cleft (**BU1**) based on the *cis* diastereomer of a rigid isophorone-derived spacer forms solid-state inclusion complexes with a range of small molecular guests. Larger guests can be accommodated by a shift in orientation to open up crystalline channels while retaining the same overall hydrogen-bonded topology. The introduction of molecular flexibility to give **BU2**, which possesses a methylene spacer, destroys the host−guest complexation behavior and restores the more conventional urea α-tape packing, giving viscous solutions due to columnar aggregation. Crystallization of both **BU1** and **BU2** from a mixture of *cis* and *trans* diastereomeric forms is highly diastereoselective with the *cis* isomers being significantly less soluble. Isolation of a *trans* isomer of **BU2** from crystallization of *cis*-depleted mother liquor reveals an unusual intramolecular hydrogen bond arrangement, explaining its greater solubility.

INTRODUCTION

Molecular clefts, clips, and tweezers are a type of receptor featuring two guest-binding domains and are typically somewhat rigid, acyclic systems with a well-defined backbone spacer geometry resulting in a controlled, but somewhat flexible, binding site geometry. Broadly, the ability of the binding pocket to surround the guest increases going from molecular clefts to clips to tweezers (Figure 1), but the concepts are closely related. Formally, the systems have "bond angle distortions", which require little energy and, therefore, should induce a certain flexibility, allowing the receptor "arms" to be expanded and compressed during the substrate complexation".[1] This setup allows the guest molecule to be held between the two "pincer arms" of the host. Molecular clefts require (i) a spacer that prevents self-association, (ii) a spacer that maintains a distance of at least about 7 Å between the pincers, suitable for accommodating a guest molecule, and (iii) a spacer that holds the two pincer arms rigidly in a *syn* type of conformation.[2] Usually, aromatic rings or alkynes serve as rigid spacers to ensure that the pincers of the host remain at the required distance apart. The concept originates from the work of Chen and Whitlock in 1978[3] inspired by the observation, in 1970, that the hydrolysis of aspirin in water is inhibited by caffeine and hence there must be some hydrophobic binding.[2] It has remained enduringly popular ever since.[2,4] Examples include recent work on acyclic glycoluril-based receptors,[5] double recognition of guests by receptors incorporating $\pi-\pi$ stacking arms and an additional hydrogen bonding core functionality,[6] and versatile series of rigid molecule clip hosts based on Kemp's triacid.[7] A characteristic of molecular clefts is their ability to flex and adapt their binding pocket according to guest size and shape, and a receptor based on methylene-bridged six-membered rings reported by Klärner and co-workers[8] is able to squeeze down from a separation of approximately 10 Å in the absence of guest to 7.6 Å when an electron-deficient aromatic guest is sandwiched between the electron-rich aromatic pincers. Other common, rigid back-

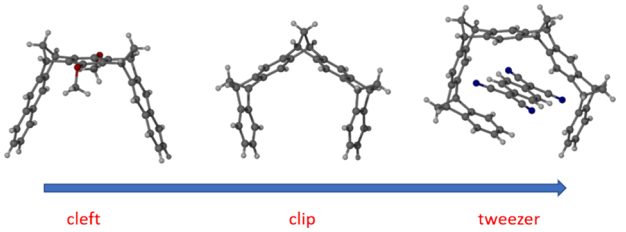

Figure 1. Loose progression from molecular clefts to clips to tweezers (the latter binding tetracyanoquinoline guest; reproduced with permission from ref 2. Copyright 2022 Wiley-Blackwell).

Received: July 4, 2024
Revised: August 15, 2024
Accepted: August 16, 2024
Published: August 21, 2024

bones include the chiral Tröger's base[9] and the Kagan's ether scaffold studied extensively by Harmata.[10]

Much of the interest in molecular clefts has been in their use in solution-phase guest binding. As examples of "awkwardly shaped" molecules with an intrinsic void space,[11] molecular clefts might also be expected to form solid-state inclusion or clathrate complexes in which the molecular cavity is occupied by coformers or guest molecules such as solvents or gases. While self-inclusion might reduce the space available for guest binding, the rigid, open V-shape of molecular clefts may reduce the self-inclusion tendency, particularly if the cleft opening is held apart by hydrogen bonding interactions in the solid state. One of the most spectacular demonstrations of this kind of principle is the recent prediction and experimental realization of a porous solid phase of an extended benzimidazolone host, which has a low density open hexagonal pore structure. The 2.8 nm wide hexagonal channels represent the largest pores found so far in an organic material, and the density of the empty apohost phase of this "organic molecule of intrinsic microporosity" (OMIM) is just 0.303 g cm^{-1}.[12]

In the present work, we report initial studies on a series of molecular cleft materials based on a rigid isophorone-derived spacer. Isophorone is found naturally in cranberries and has a peppermint-like odor.[13] Isophorone diisocyanate is a cheap, commercially available derivative and is a common polymer precursor. In addition to its rigid, cyclic aliphatic structure, the isophorone backbone is unsymmetrical, giving rise to the possibility of enhanced selectivity and directional binding. The two isocyanate groups have different reactivities, with the primary being more reactive than the secondary isocyanate group, suggesting the possibility of further desymmetrization. Isophorone has been used as the basis for bis(acyl-semicarbazide) fatty acid gelators that computational and IR studies indicate intramolecular hydrogen bonding and no open molecular cleft.[14] In this case, we focus on the derivatization of isophorone diisocyanate to give sterically hindered urea-based pincer arms, which have been shown previously to give interesting clathrate structures[15] and have been incorporated into the molecular cleft and MOF materials for solid-state anion recognition.[16,17]

RESULTS AND DISCUSSION

Synthesis and Design. Two new bis(urea) molecular clefts (**BU1** and **BU2**; Scheme 1) were prepared by the straightforward reaction of isophorone diisocyanate with either 3-aminopyridine or 3-aminomethylpyridine in a 1:2 stochiometric ratio. After solvent evaporation, the resultant white powders were washed with boiling water to remove impurities and characterized by ^{1}H and $^{13}C\{^{1}H\}$ NMR spectroscopy, FT-IR spectroscopy, elemental analysis, and single-crystal X-ray diffraction (see the Supporting Information).

Scheme 1. Molecular Clefts Prepared in This Work[a]

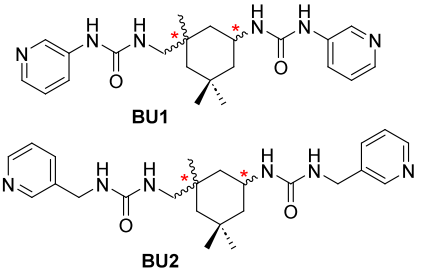

[a]Chiral centers are marked with an asterisk. Both compounds were prepared as diastereomeric mixtures with either *cis* (RS/SR) or *trans* (RR/SS) relative disposition of the two urea arms.

The urea functional groups in **BU1** and **BU2** are rigid and planar and offer the possibility of a well-defined hydrogen-bonded channel by formation of the common urea α-tape hydrogen-bonded motif.[18−22] The pyridyl group in **BU1** extends the rigid structure to give a significant molecular cleft. The occurrence of intramolecular CH···O hydrogen bonding interaction in pyridyl ureas of this type, from the activated pyridyl CH group to the urea carbonyl oxygen atom,[22] is expected to planarize the entire pincer unit and reduce the tendency toward gel formation common in bis(ureas).[23−26] For comparison, the methylene spacer in **BU2** is likely to impart significantly more molecular flexibility.

The isophorone backbone possesses two chiral centers and occurs as a mixture of *cis* and *trans* diastereoisomers (each of which exists as two enantiomers). While the 1,3-substitution pattern of the cyclohexenyl ring ensures that the two pyridyl urea pincers tend toward a cleft-like arrangement, the *cis* isomer is expected to direct the pincer arms parallel to one another, while the *trans* isomer may be less effective. The evaporation and washing workup adopted are not expected to bring about any selective precipitation of either diastereoisomer.

Solid-State Host−Guest Chemistry. The propensity of molecular cleft **BU1** to form solid-state host−guest complexes was examined by crystallization by using an extensive solvent screen. **BU1** was screened with 34 different solvents at 1% and 2 wt % and dissolved in 15 cases. Saturated solutions were identified at the concentration at which the compound remained in solution for a few hours, and if more **BU1** was dissolved into solution, then it would cause precipitation. The concentration of **BU1** was increased for better solvents, namely, ethanol, methanol, cyclopentanone, 2-picoline, 1-propanol, and 2-propanol, to reach saturation. The concentration of **BU1** was lowered in solutions, which resulted in precipitates, namely, nitrobenzene, THF, and 1,4-dioxane. Crystallization was attempted by both slow cooling from heated solutions and by slow evaporation. These experiments resulted in four samples suitable for single-crystal structure determination from acetone, ethanol, cyclopentanone, and nitrobenzene. Two different habits of crystal were noted from ethanol solution; however, both proved to be the same form upon crystallographic analysis (Figure 2).

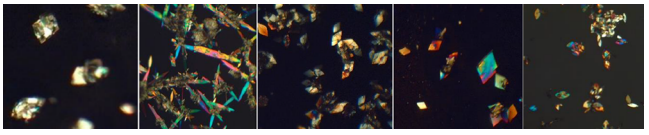

Figure 2. From left to right: crystals of **BU1** from ethanol (square plates) 10%, ethanol (needles) 10%, acetone 1%, cyclopentanone 1%, and nitrobenzene 1%.

Analysis of these samples by single-crystal X-ray diffraction showed that **BU1** forms host−guest complexes in every case, with the guest molecules sandwiched between the pincer arms of the **BU1** cleft (Figure 3a). In every structure, it is the *cis* (RS/SR diastereoisomer) that crystallizes, indicating that this is the less soluble form. This issue is discussed in detail under the Isomeric Selectivity section below. The crystals exist as two

https://doi.org/10.1021/acs.cgd.4c00928
Cryst. Growth Des. 2024, 24, 7271−7277

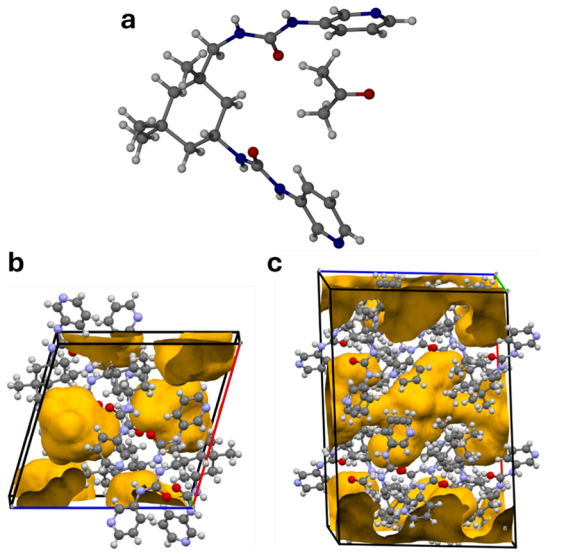

Figure 3. (a) Acetone cleft inclusion complex of **BU1**. (b) Discrete cavities containing solvent guests in Type I. (c) Linked voids containing nitrobenzene in the Type II complex of **BU1**.

different solid form types. Type I crystals (acetone, ethanol, and cyclopentanone) adopt space group $P2_1/n$ with a 1:1 host–guest stoichiometry (confirmed by solution ^{1}H NMR spectroscopy), while the nitrobenzene complex is Type II in $C2/c$ with a 4:3 stoichiometry. While the nitrobenzene guests and the host itself in the Type II crystal are highly disordered, the guests are situated within the molecular cleft. The difference in packing lies in the large size of the nitrobenzene that lies in a continuous series of linked voids formed by pairs of cleft hosts along the crystallographic c axis (Figure 3c). The solvent channel occupies 1012 Å^3 per unit cell, or 18.8% of the cell volume according to the Mercury void calculation.[27] In contrast, the other smaller solvent molecules fit well within the molecular cleft as exemplified by the acetone structure (Figure 3b), and the guests sit within discrete voids in the Type I structure. The overall void volume is 474 Å^3 per cell, or 19% of cell volume, very similar to Type II. Thus, the larger guest in Type II is accommodated by a shift to a continuous channel with lower occupancy rather than an expansion of the host structure. While a good fit for the cleft, each Type I guest exhibits two- or three-fold orientational disorder highlighting the lack of specific interactions between the guest and cleft.

In both types of solvates, the dominant packing motif comprises hydrogen-bonded dimeric pairs linked on the less sterically hindered face of the isophorone linker unit. The urea groups are antiparallel, and dimers are linked by two classic, symmetrical $R_2^1(6)$ urea hydrogen-bonded motifs (Figure 4a), with N···O distances of around 2.9 Å.[20,21] The much more hindered opposite face in both Type I and Type II adopts a more complex hydrogen bonding mode with the two urea NH groups hydrogen bonding to either the carbonyl oxygen atom of an adjacent molecule or the pyridyl nitrogen atom on a different adjacent molecule giving an overall much larger second-level graph set[28] pattern $R_4^4(22)$ (Figure 4b). Urea-pyridyl hydrogen bonding in related systems is common because of the hindrance of the urea carbonyl caused by intramolecular CH···O hydrogen bonds,[22] and this motif corresponds to the arrangement termed intermediate non-bifurcated urea-pyridyl synthon VI.[19]

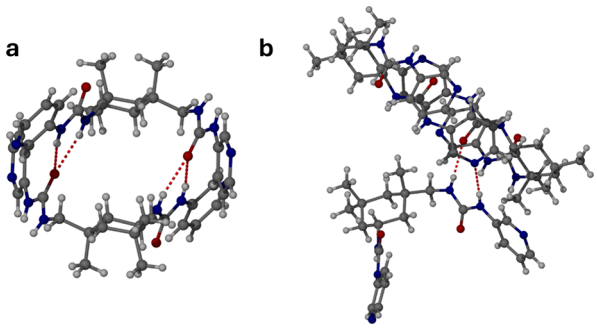

Figure 4. (a) Symmetrical dimer formation on the less sterically hindered face of cleft **BU1** in both types of complexes. N···O distances for the acetone solvate: 2.883(3) and 2.890(4) Å. (b) Part of the nonbifurcated urea-pyridyl synthon VI pattern that gives rise to a $R_4^4(22)$ motif on the more hindered cleft face. N···O 2.873(3) and N···N 2.977(4) Å. The same motifs are observed in all four structures.

The size of the cleft can be assessed by measurement of the intercentroid distance between the terminal pyridyl groups and is remarkably constant across all four structures of both types with distances of 8.93, 9.06, 9.16, and 8.84 Å for the Type I acetone, cyclopentanone, ethanol, and Type II nitrobenzene structures, respectively. This highlights the rigidity of the cleft geometry.

Flexible Alternative Host. The more flexible **BU2** acts as a control compound since, unlike **BU1**, it does not possess a rigidly preorganized molecular cleft. **BU2** is more soluble than **BU1** and dissolves in 28 of the 34 solvents tested. Crystallization was also attempted in solvent mixtures by slow cooling and slow evaporation. These experiments resulted in two samples of **BU2** suitable for single-crystal X-ray analysis: a chloroform solvate and an apparently nonsolvated form (Figure 5a,b). Both were analyzed by single-crystal XRD. The acicular habit and small size of the nonsolvated form required the use of the I19 beamline at the Diamond synchrotron.[29]

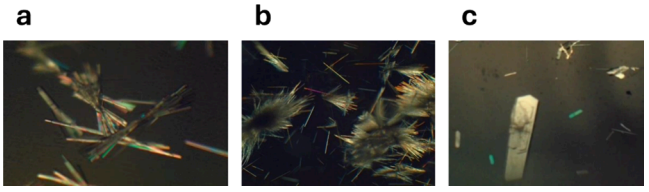

Figure 5. Crystals of **BU2** isolated from (a) chloroform (*cis* chloroform solvate), (b) acetone (*cis* nonsolvated form), and (c) from the acetone mother liquor (*trans* nonsolvated form).

Unlike **BU1**, compound **BU2** does not function as a molecular cleft in either of the forms isolated, and in both cases, the ostensible cleft position is filled by self-inclusion of one of the pyridyl groups facilitated by the flexible methylene spacer (Figure 6a). Both structures adopt a more conventional double urea α-tape packing arrangement,[30] which involves face-to-face stacking similar to that seen in the **BU1** structures as well as similar stacking on the opposite face to give molecular columns, albeit with somewhat unsymmetrical bifurcated acceptor N···O interactions ranging from 2.89 to 3.1 Å (Figure 6b). In the chloroform solvate, the chloroform guests hydrogen bond with pyridyl nitrogen atoms on the outside of the molecular stack. In the nonsolvated structure, this pyridyl group is disordered and there remains 182 Å^3 (3.8%) of an accessible void space indicating "awkward"

https://doi.org/10.1021/acs.cgd.4c00928
Cryst. Growth Des. 2024, 24, 7271−7277

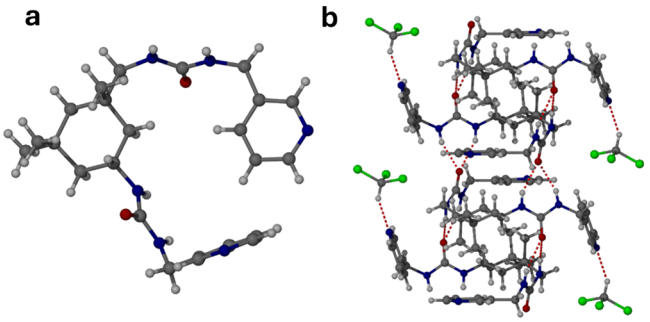

Figure 6. (a) Molecular structure of **BU2** in chloroform solvate. (b) Double urea α-tape columnar packing arrangement in the **BU2** structures (chloroform solvate shown). N···O distances 2.885(2), 2.953(2), 2.978(2), and 3.119(2) Å. Cl_3HC···N 3.213(2) Å. In the unsolvated structure, the pyridyl group is disordered and 3.8% void space remains.

packing or possibly unresolved residual channel solvent. While both solvated and unsolvated forms have a similar 9.2 Å unit cell axis corresponding to the urea α-tape column, the desolvated form is high-symmetry tetragonal $P4_2/n$ while the chloroform solvate is triclinic $P\bar{1}$.

Isomeric Selectivity. Remarkably, it is the *cis* or RS/SR diastereoisomer rather than the *trans* RR/SS form that is observed in all of the **BU1** and **BU2** cleft structures. This is fortuitous since this isomer is expected to have more parallel pincer arms and hence function more effectively as a cleft. The isophorone diisocyanate starting material exists as a mixture of both diastereomeric forms. While the existence of two diastereoisomers is not clear from the solution ^{1}H NMR spectroscopic data for **BU1** and **BU2**, it is likely that both forms have similar chemical shifts, and there is no reason to expect diastereoselectivity in the synthetic procedure. To assess isomeric purity and determine whether the single-crystal structures are representative of the bulk material, XRPD analysis was undertaken on all samples.

The powder patterns of the **BU1** solvates with ethanol, acetone, and cyclopentanone guests display the same peaks in their experimental patterns as their calculated powder patterns derived from the single-crystal data. Hence, the single-crystal data is representative of the bulk, and the crystallization occurs diastereoselectively. An additional set of broad peaks can be identified in the powder pattern of the as-synthesized **BU1** material, which is prepared by evaporation of the solvent, compared with the XRPD patterns of the ethanol, acetone, and cyclopentanone recrystallized samples. This additional set of peaks (Figure 7a, arrows) is likely to be representative of the *trans* diastereoisomer present in the "as-synthesized" **BU1** powder before recrystallization. Small shifts in peak positions reflect the different temperatures of the low-temperature single-crystal data compared to the room temperature XRPD measurement and likely different solvent occupancy of the as-synthesized **BU1** compared to the recrystallized samples, although it is apparent that the *cis* isomer in the as-synthesized material has a Type I structure. The nitrobenzene sample is the alternative Type II solvatomorph, and the experimental XRPD pattern appears to be significantly affected by preferred orientation leading, for example, to the very low intensity of the (110) peak at 8.2° 2θ (Figure 7).

In the case of **BU2**, again, the single crystal appears to represent the bulk recrystallized material in both the chloroform solvate and unsolvated products and hence is

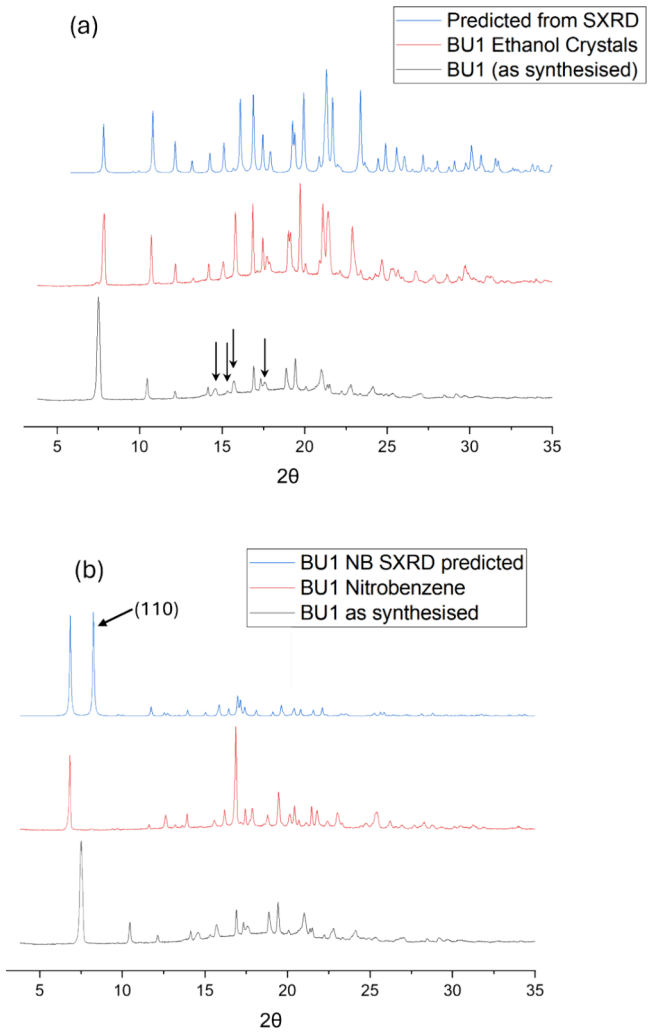

Figure 7. X-ray powder diffraction patterns of **BU1** recrystallized from (a) ethanol and (b) nitrobenzene compared to the calculated patterns from the low-temperature single-crystal data and the "as-synthesized" material. Arrows in the "as-synthesized" pattern point to additional peaks that may represent the *trans* diastereoisomer. The experimental intensity of the (110) reflection in particular appears to be significantly affected by the preferred orientation.

free of the *trans* diastereoisomer, albeit again with considerable preferred orientation effects as would be anticipated from the extreme acicular morphology of the samples (Figure 5a,b). The XRPD pattern of the as-synthesized material resembles that of the chloroform solvate (indeed, the compound is prepared using chloroform) but with additional peaks suggesting the presence of a second diastereoisomer (Figure 8).

The disappearance of this second *trans* diastereoisomer on recrystallization implies that it is considerably more soluble for both **BU1** and **BU2**. To establish this point and rule out the *trans* isomer as a potentially useful molecular cleft, the *cis* nonsolvated crystals of **BU2** were removed from the acetone mother liquor by filtration and the remaining solution was left to slowly evaporate over a week. This led to the formation of another set of crystals with a tabular habit (Figure 5c). Single-crystal X-ray analysis of this sample revealed it to be an unsolvated form of the previously unobserved *trans* isomer. The structure immediately provides a reason for the compound's greater solubility since it involves the relatively unusual[31] *syn*−*anti* conformation of one of the two urea groups

https://doi.org/10.1021/acs.cgd.4c00928
Cryst. Growth Des. 2024, 24, 7271−7277

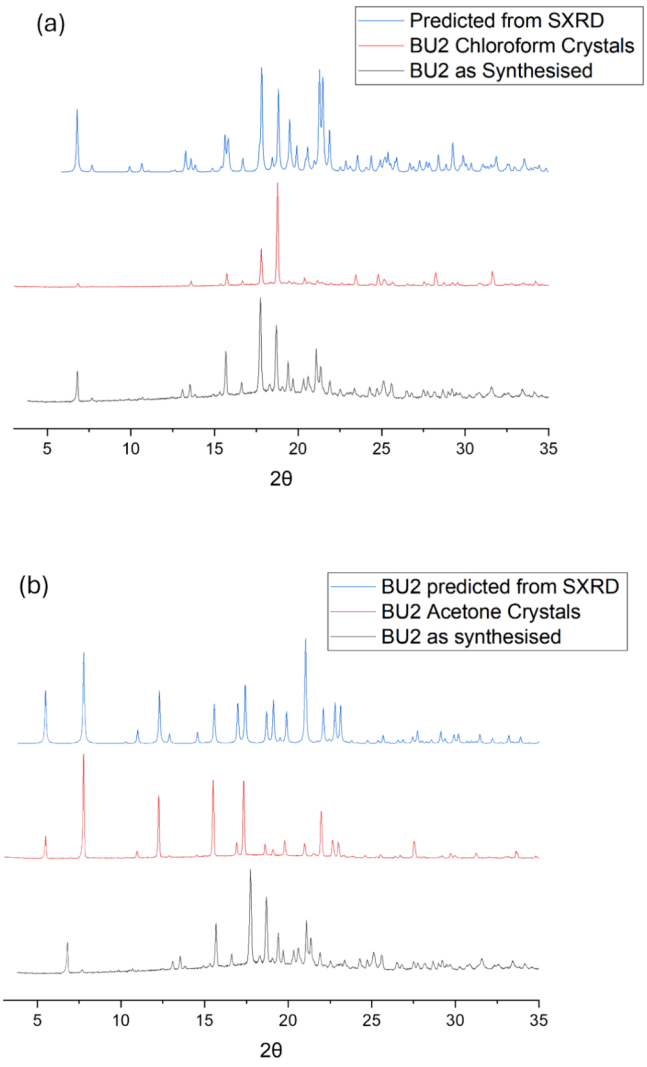

Figure 8. X-ray powder diffraction patterns of **BU2** recrystallized from (a) chloroform and (b) acetone (unsolvated form) compared to the calculated patterns from the low-temperature single-crystal data and the "as-synthesized" material.

and the formation of an intramolecular hydrogen bond, N···O 2.88 Å. This allows the formation of an eight-membered $R_2^2(8)$ intermolecular hydrogen-bonded ring motif. The other urea group is in the more common *anti*−*anti* conformation but is highly sterically hindered, preventing the formation of the conventional coplanar $R_2^1(6)$ motif. Instead, this group is situated perpendicular to the *syn*−*anti* urea hydrogen-bonded dimer giving a very unusual, perpendicular interaction (Figure 9), with relatively long N···O distances of 2.97 and 3.09 Å. The greatly reduced intermolecular hydrogen bonding in this *trans* form is expected to result in lower crystal stability and hence reduced solubility. The Uni intermolecular potential tool in Mercury[32,33] gives an overall packing energy for this structure of −252.6 kJ mol^{-1} compared to the chloroform solvate *cis* isomer of **BU2** of −302.9 kJ mol^{-1}. The unfilled void space in the nonsolvated form of the *cis* compound results in a nonsensical calculated packing energy of +124.3 kJ mol^{-1}. The SQUEEZE procedure[34] indicates that this void space is genuinely empty with no residual electron density.

Gelation Behavior. Bis(urea) compounds commonly give rise to low molecular weight supramolecular gels in various

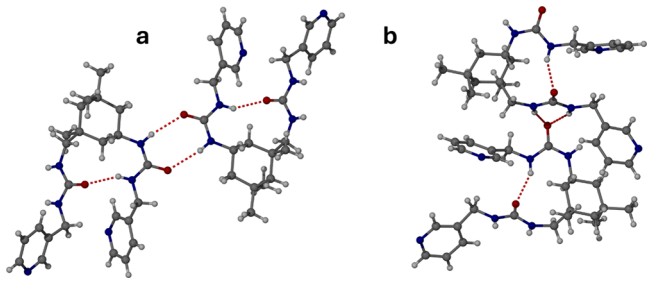

Figure 9. X-ray crystal structure of *trans*-**BU2** showing the intramolecular hydrogen bonding, the *syn*−*anti* conformation of one of the urea groups that results in (a) an $R_2^2(8)$ intermolecular hydrogen-bonded ring motif, and (b) the highly sterically hindered, perpendicular $R_2^1(6)$ motif.

solvents.[24,26,30,35,36] Gel formation is often associated with the formation of self-assembled fibrillar nanostructures (SAFiNs)[37−39] via the urea α-tape hydrogen-bonded motif. No gel formation was observed during this study, which may be correlated with the lack of α-tape hydrogen bonding in both types of the **BU1** structure. While also a nongelator, **BU2** formed very viscous liquids with water at 1−4% by weight. At 5 wt %, however, **BU2** precipitated. Similar results were obtained with mixtures at different wt % of **BU2** in water and THF at a 3:2 ratio. These solutions became more viscous as the THF evaporated; however, no gels were observed. Similarly, neither sonication nor shaking induced gelation in any of the solutions or viscous liquid samples. Preliminary attempts were also made to induce gelation by addition of copper(II) salts.[36] Copper salts were combined into solutions in which the salts are soluble (e.g., water, THF, *etc.*) by first dissolving the metal salt in a minimum amount of the solvent (0.01 mL) and then adding the salt solution to the saturated solution of **BU2**. Alternatively, the salt was dissolved in a minimum amount of methanol and then added to the saturated solution of solvents in which metal salts are not soluble (e.g., nitrobenzene). While no metallogels were formed, the addition of $Cu(BF_4)_2$ and $CuCl_2$ at 0.5 mol equiv in 3:2 water:THF at 2% and 4 wt % of **BU2** appeared to give rise to materials that pass the common "inversion test" for gels.[40,41] However, these materials proved not to be gels, and the lack of liquid flow was caused by the formation of a solid skin across the surface of the samples, likely prompted by the evaporation of THF from the solution mixture and some minimal gel-like aggregation. The SEM images of the freeze-dried "gel-like" samples displayed the absence of any gel fibers, and the material beneath the skin remained liquid (Figures S1 and S2).

CONCLUSIONS

The rigid molecular cleft geometry of **BU1** induced by the asymmetric isophorone-derived backbone prevents the formation of the well-known urea α-tape hydrogen-bonded motif and simultaneously creates a well-defined guest-binding pocket. This results in hydrogen-bonded dimers in the solid state that is associated with the unusual nonbifurcated urea-pyridyl synthon VI pattern[19] and gives rise to consistent inclusion complex formation with small molecular guests such as acetone, ethanol, and cyclopentanone. The pattern can be adapted to give Type II channel structures the ability to incorporate larger guests such as nitrobenzene. The crystallization of both **BU1** and **BU2** is strongly diastereoselective with the less soluble *cis* diastereoisomers being observed in

https://doi.org/10.1021/acs.cgd.4c00928
Cryst. Growth Des. 2024, 24, 7271−7277

every case. For at least **BU2**, the *trans* isomer may be obtained from the mother liquor after removal of the *cis* form, and its higher solubility appears to arise from the formation of intramolecular hydrogen bonding and an unusual, perpendicular distorted hydrogen-bonded arrangement. The introduction of additional flexibility as in **BU2** restores the α-tape packing motif and results in the beginnings of molecular aggregation to give viscous solutions, if not complete, gelation behavior. Finally, this work highlights the warning[40] that samples that pass the simple inversion test may well not be gels, and liquid may be trapped under a thin solid layer.

■ ASSOCIATED CONTENT

Supporting Information

The Supporting Information is available free of charge at https://pubs.acs.org/doi/10.1021/acs.cgd.4c00928.

Synthetic details and photographs of samples as well as SEM images of the nongelled samples and X-ray crystallographic information; underlying data for this work comprising raw NMR, IR, XRPD, and elemental analysis (PDF)

Data can be obtained from DOI: 10.15128/r28910jt63h

Accession Codes

CCDC 2367703−2367709 contain the supplementary crystallographic data for this paper. These data can be obtained free of charge via www.ccdc.cam.ac.uk/data_request/cif, or by emailing data_request@ccdc.cam.ac.uk, or by contacting The Cambridge Crystallographic Data Centre, 12 Union Road, Cambridge CB2 1EZ, UK; fax: +44 1223 336033.

■ AUTHOR INFORMATION

Corresponding Author

Jonathan W. Steed − *Department of Chemistry, Durham University, Durham DH1 3LE, U.K.;* orcid.org/0000-0002-7466-7794; Email: jon.steed@durham.ac.uk

Authors

Abbie V. Lynch − *Department of Chemistry, Durham University, Durham DH1 3LE, U.K.*

Toby J. Blundell − *Department of Chemistry, Durham University, Durham DH1 3LE, U.K.;* orcid.org/0000-0002-7296-1471

Complete contact information is available at: https://pubs.acs.org/10.1021/acs.cgd.4c00928

Author Contributions

The manuscript was written through contributions of all authors. All authors have given approval to the final version of the manuscript. A.V.L. carried out the experimental work, T.J.B. carried out the crystallographic analyses, and J.W.S. conceived and designed the project.

Notes

The authors declare no competing financial interest.

■ ACKNOWLEDGMENTS

We thank Durham University for provision of facilities and the SFTC. We would like to thank Diamond Light Source for an award of instrument time on Station I19 under BAG proposal CY30280 as well as beamline scientists Dr. Sarah Barnett and Dr. Dave Allan for support.

■ REFERENCES

(1) Klärner, F. G.; Kahlert, B. Molecular tweezers and clips as synthetic receptors. Molecular recognition and dynamics in receptor-substrate complexes. *Acc. Chem. Res.* **2003**, *36*, 919−932.

(2) Steed, J. W.; Atwood, J. L. *Supramolecular Chemistry*. 3rd ed.; Wiley-Blackwell: Chichester, 2022.

(3) Chen, C. W.; Whitlock, H. W. Molecular Tweezers - Simple-Model of Bifunctional Intercalation. *J. Am. Chem. Soc.* **1978**, *100*, 4921−4922.

(4) Hardouin-Lerouge, M.; Hudhomme, P.; Sallé, M. Molecular clips and tweezers hosting neutral guests. *Chem. Soc. Rev.* **2011**, *40*, 30−43.

(5) Ganapati, S.; Isaacs, L. Acyclic Cucurbit[n]uril-type Receptors: Preparation, Molecular Recognition Properties and Biological Applications. *Israel J. Chem.* **2018**, *58*, 250−263.

(6) Zimmerman, S. C. Rigid Molecular Tweezers as Hosts for the Complexation of Neutral Guests. *Top. Curr. Chem.* **1993**, *165*, 71−102.

(7) Rebek, J. Molecular Recognition with Model Systems. *Angew. Chem., Int. Ed. Engl.* **1990**, *29*, 245−255.

(8) Klärner, F. G.; Panitzky, J.; Blaser, D.; Boese, R. Synthesis and supramolecular structures of molecular clips. *Tetrahedron* **2001**, *57*, 3673−3687.

(9) Adrian, J. C.; Wilcox, C. S. Chemistry of Synthetic Receptors and Functional-Group Arrays 0.15. Effects of Added Water on Thermodynamic Aspects of Hydrogen-Bond-Based Molecular Recognition in Chloroform. *J. Am. Chem. Soc.* **1991**, *113*, 678−680.

(10) Hamata, M. Chiral molecular tweezers. *Acc. Chem. Res.* **2004**, *37*, 862−873.

(11) Das, D.; Chuskit, S.; Shrivastava, A.; Dwivedi, B. Versatile Solid-State Inclusion Property of a New Bis-hydrazone Compound. *Cryst. Growth Des.* **2023**, *23*, 8043−8051.

(12) Pulido, A.; Chen, L.; Kaczorowski, T.; Holden, D.; Little, M. A.; Chong, S. Y.; Slater, B. J.; McMahon, D. P.; Bonillo, B.; Stackhouse, C. J.; Stephenson, A.; Kane, C. M.; Clowes, R.; Hasell, T.; Cooper, A. I.; Day, G. M. Functional materials discovery using energy−structure−function maps. *Nature* **2017**, *543*, 657.

(13) Siegel, H.; Eggersdorfer, M.; Ketones. In *Ullmann's Encyclopedia of Industrial Chemistry* Wiley-VCH Verlag GmbH & Co. KGaA 2000.

(14) Baddi, S.; Madugula, S. S.; Sarma, D. S.; Soujanya, Y.; Palanisamy, A. Combined Experimental and Computational Study of the Gelation of Cyclohexane-Based Bis(acyl-semicarbazides) and the Multi-Stimuli-Responsive Properties of Their Gels. *Langmuir* **2016**, *32*, 889−899.

(15) Todd, A. M.; Anderson, K. M.; Byrne, P.; Goeta, A. E.; Steed, J. W. Helical or polar guest-dependent Z ′=1.5 or Z ′=2 forms of a sterically hindered bis(urea) clathrate. *Cryst. Growth Des.* **2006**, *6*, 1750−1752.

(16) Biswas, R.; Ghorai, S.; Paul, B.; Maji, S.; Natarajan, R. Cleft Receptor for the Recognition and Extraction of Tetrahedral Oxyanions. *Cryst. Growth Des.* **2023**, *23*, 4384−4394.

(17) Mondal, P. P.; Muthukumar, D.; Fathima, S. K. P.; Pillai, R. S.; Neogi, S. Interpenetrated Robust Metal-Organic Framework with Urea-Functionality-Decked Pores for Selective and Ultrasensitive Detection of Antibiotics and Oxo-anions. *Cryst. Growth Des.* **2023**, *23*, 8342−8351.

(18) van Esch, J.; De Feyter, S.; Kellogg, R. M.; De Schryver, F.; Feringa, B. L. Self-Assembly of Bisurea Compounds in Organic Solvents and on Solid Substrates. *Chem.—Eur. J.* **1997**, *3*, 1238−1243.

(19) Byrne, P.; Turner, D. R.; Lloyd, G. O.; Clarke, N.; Steed, J. W. Gradual transition from NH···pyridyl hydrogen bonding to the NH···O tape synthon in pyridyl ureas. *Cryst. Growth Des.* **2008**, *8*, 3335−3344.

(20) Etter, M. C. Encoding and Decoding Hydrogen Bond Patterns of Organic Compounds. *Acc. Chem. Res.* **1990**, *23*, 120−126.

(21) Etter, M. C.; Urbanczyk-Lipkowska, Z.; Zia-Ebrahimi, M.; Panunto, T. W. Hydrogen Bond Directed Cocrystallization and Molecular Recognition Properties of Diaryl Ureas. *J. Am. Chem. Soc.* **1990**, *112*, 8415−8426.

(22) Reddy, L. S.; Basavoju, S.; Vangala, V. R.; Nangia, A. Hydrogen bonding in crystal structures of N,N'-bis(3-pyridyl)urea. Why is the N-H···O tape synthon absent in diaryl ureas with electron-withdrawing groups? *Cryst. Growth Des.* **2006**, *6*, 161−173.
(23) Lloyd, G. O.; Piepenbrock, M. O. M.; Foster, J. A.; Clarke, N.; Steed, J. W. Anion tuning of chiral bis(urea) low molecular weight gels. *Soft Matter* **2012**, *8*, 204−216.
(24) Fernandez-Prieto, S.; Miravet-Celades, J.; Ojeda-Flores, J.-J.; Johan, S.; Urea Gellants. WO2016209785A1, 2016.
(25) Van Lommel, R.; Rutgeerts, L. A. J.; De Borggraeve, W. M.; De Proft, F.; Alonso, M. Rationalising Supramolecular Hydrogelation of Bis-Urea-Based Gelators through a Multiscale Approach. *ChemPlusChem.* **2020**, *85*, 267−276.
(26) Yokoya, M.; Kimura, S.; Yamanaka, M. Urea Derivatives as Functional Molecules: Supramolecular Capsules, Supramolecular Polymers, Supramolecular Gels, Artificial Hosts, and Catalysts. *Chem.—Eur. J.* **2021**, *27*, 5601−5614.
(27) Macrae, C. F.; Sovago, I.; Cottrell, S. J.; Galek, P. T. A.; McCabe, P.; Pidcock, E.; Platings, M.; Shields, G. P.; Stevens, J. S.; Towler, M.; Wood, P. A. Mercury 4.0: from visualization to analysis, design and prediction. *J. Appl. Crystallogr.* **2020**, *53*, 226−235.
(28) Bernstein, J.; Davis, R. E.; Shimoni, L.; Chang, N. L. Patterns in hydrogen bonding - functionality and graph set analysis in crystals. *Angew. Chem., Int. Ed.* **1995**, *34*, 1555−1573.
(29) Nowell, H.; Barnett, S. A.; Christensen, K. E.; Teat, S. J.; Allan, D. R. I19, the small-molecule single-crystal diffraction beamline at Diamond Light Source. *Journal of Synchrotron Radiation* **2012**, *19*, 435−441.
(30) van Esch, J. H.; Schoonbeek, F.; de Loos, M.; Kooijman, H.; Spek, A. L.; Kellogg, R. M.; Feringa, B. L. Cyclic Bis-Urea Compounds as Gelators for Organic Solvents. *Chem.—Eur. J.* **1999**, *5*, 937−950.
(31) Foster, J. A.; Damodaran, K. K.; Maurin, A.; Day, G. M.; Thompson, H. P. G.; Cameron, G. J.; Bernal, J. C.; Steed, J. W. Pharmaceutical polymorph control in a drug-mimetic supramolecular gel. *Chem. Sci.* **2017**, *8*, 78−84.
(32) Gavezzotti, A. Are Crystal Structures Predictable? *Acc. Chem. Res.* **1994**, *27*, 309−314.
(33) Gavezzotti, A.; Filippini, G. Geometry of the Intermolecular X-H.cntdot..cntdot..cntdot.Y (X, Y = N, O) Hydrogen Bond and the Calibration of Empirical Hydrogen-Bond Potentials. *J. Phys. Chem.* **1994**, *98*, 4831−4837.
(34) Spek, A. PLATON SQUEEZE: a tool for the calculation of the disordered solvent contribution to the calculated structure factors. *Acta Crystallogr. Sect. C* **2015**, *71*, 9−18.
(35) Fages, F.; Vögtle, F.; Žinic, M. Systematic Design of Amide- and Urea-Type Gelators with Tailored Properties. *In Top. Curr. Chem.* **2005**, *256*, 77−131.
(36) Byrne, P.; Lloyd, G. O.; Applegarth, L.; Anderson, K. M.; Clarke, N.; Steed, J. W. Metal-Induced Gelation in Dipyridyl Ureas. *New J. Chem.* **2010**, *34*, 2261−2274.
(37) Mallia, V. A.; Weiss, R. G. Correlations between thixotropic and structural properties of molecular gels with crystalline networks. *Soft Matter* **2016**, *12*, 3665−3676.
(38) Huang, X.; Raghavan, S. R.; Terech, P.; Weiss, R. G. Distinct kinetic pathways generate organogel networks with contrasting fractality and thixotropic properties. *J. Am. Chem. Soc.* **2006**, *128*, 15341−15352.
(39) Terech, P.; Weiss, R. G. Low Molecular Mass Gelators of Organic Liquids and the Properties of Their Gels. *Chem. Rev.* **1997**, *97*, 3133−3160.
(40) Draper, E. R.; Adams, D. J. How should multicomponent supramolecular gels be characterised? *Chem. Soc. Rev.* **2018**, *47*, 3395−3405.
(41) Adarsh, N. N.; Kumar, D. K.; Dastidar, P. Cu^{II} coordination polymers derived from bis-pyridyl-bis-urea ligands: synthesis, selective anion separation and metallogelation. *Curr. Sci.* **2011**, *101*, 869−880.

https://doi.org/10.1021/acs.cgd.4c00928
Cryst. Growth Des. 2024, 24, 7271−7277